JOURNAL OF MATERIALS SCIENCE 8 (1973) 1153–1164

A comparative study of the fracture of various silica modifications using the Hertzian test

M. V. SWAIN, J. S. WILLIAMS, B. R. LAWN, J. J. H. BEEK
School of Physics, University of New South Wales, Kensington, NSW, Australia

A comprehensive Hertzian fracture study has been made of quartz, fused silica and soda-lime glass. The two main aspects are: (i) vacuum tests, which reflect the intrinsic bond strength of the –Si–O– network, and (ii) water-environment tests, which reflect the rate processes involved in hydrolytic bond weakening. Temperature, load rate and chemical concentration are the variables investigated. The incorporation of new features into the elementary Si–O bond-rupture picture of crack extension is necessary to account for the results. In vacuum, the Hertzian fracture strength of quartz decreases dramatically as the $\alpha \rightarrow \beta$ inversion temperature is approached; no such effect is evident in the non-crystalline modifications. This result is interpreted in terms of thermal oscillations of the stacking tetrahedra in the SiO_2 structure. In water environments, the Hertzian strength is universally depressed, the effect becoming more pronounced at low load rates, high chemical concentrations. The physical state of the environment is an important factor in the kinetics of the hydrolytic weakening process: with the liquid state, the (thermally-activated) reaction between water molecules and crack-tip bonds is rate-controlling; whereas with the gaseous state, it is the (temperature-insensitive) molecular diffusion along the fracture interface which controls. The secondary role of composition effects, dissipative crack-tip processes, etc., is also discussed.

1. Introduction

The brittle fracture of silicate materials has an important bearing on a wide range of disciplines, including the physics and chemistry of ceramics, engineering design, and the earth sciences. Since the pioneering work of Griffith [1] in 1920, a vast body of information has beeen amassed on the subject, particularly in connection with the fracture strength of commercial glasses [for recent reviews see refs. 2-5]. However, because of the large number of variables which enter the fracture problem, structural variations, state of specimen surface, temperature, chemical environment, stress state, etc., it is not always easy to correlate the available data. The general picture is consequently still somewhat obscure, and there appears to be a need for an inter-disciplinary, "materials science" approach.

The basic building block of silica, SiO_2, is the SiO_4^{4-} tetrahedral unit. The ordered stacking of these units gives rise to the crystal modifications of quartz; disordered stacking likewise gives the amorphous modification, fused silica. Since the tetrahedra stack corner-to-corner the structures are "open", with large interstices to accommodate impurities. The incorporation of certain "network modifiers" into the structure, as with alkali and alkaline earth ions in common silicate glasses, may have a significant effect on mechanical properties [6]. Of particular relevance to the growth of cracks is the dramatic hydrolytic weakening caused by the activated reaction of water molecules (available either internally or externally) with highly stressed –Si–O– (siloxane) bridges to form terminal –Si–OH (silanol) groups. A simplistic conception of fracture in terms of a bond-rupture process common to all forms of silica has emerged: under "dry" conditions the resistance to crack growth arises primarily from the intrinsic strength of the Si–O bond; under "wet" conditions the hydrolysis of crack-tip bonds greatly lowers this resistance, the reaction

kinetics introducing a rate-dependent element into the problem.

The purpose of this paper is a comprehensive study of the fracture behaviour of several modifications of SiO_2 under a variety of test conditions. Such a proposition would hardly be feasible using conventional fracture methods, since the time and expense involved in reproducing and testing vast numbers of test pieces (providing in most cases one result per specimen) would be prohibitive. But with the advent of the so-called Hertzian indentation test as a suitable microprobe of fracture strength [7-11], the rapid accumulation of data from relatively small, easily prepared specimens has become possible. Tests of a preliminary nature on soda-lime glass [9] and α-quartz [11] have served to demonstrate the versatility of the technique. An environmental chamber recently constructed in these laboratories has been used to regulate the test conditions in the collection of results in the present work. The investigation reveals the simple bond-rupture picture of crack growth to be incomplete, with structural variations in the silica network and the physical state of the environment playing major roles.

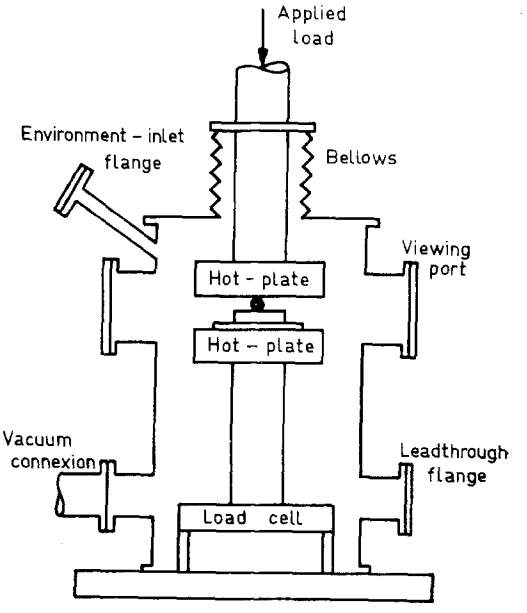

Figure 1 Environmental chamber for Hertzian fracture testing. Indenter seats on specimen between hot-plates. Only essential details are shown.

2. The Hertzian fracture test

2.1. Experimental procedure

The apparatus for controlled Hertzian fracture testing has been described elsewhere [12], and only the essential features will be pointed out here. Basically, the arrangement consists of an indentation assembly housed within an environmental chamber (Fig. 1). An externally-applied dead-weight load is transmitted to the indenter, a 13 mm diameter WC sphere, through a bellows system. The load is increased at a constant rate (available range 1 to 500 N sec^{-1}) until a cone-shaped crack, the "Hertzian cone", is seen to suddenly grow into the specimen from just outside the elastic contact circle. An internal load cell measures the critical load P_c delivered to the specimen. By manipulating an externally controlled indenter-moving device the indentation site may be rapidly changed, thereby permitting some 100 tests to be made on a typical specimen surface.

The main chamber (Fig. 1) is designed for accurate control of the test environment. A furnace and makeshift cold-finger assembly provides a working range 175 to 900 K in specimen temperature, with variations less than $\pm$ 3°. Facility exists for evacuating the chamber to better than 10^{-4} N m^{-2} (10^{-6} Torr), or for leaking in a gas or liquid environment.

Specimens of α-quartz, fused silica and soda-lime glass were prepared in slab-like form with thickness 8 to 12 mm. The surfaces were given a standard pre-abrasion treatment with a slurry of 500-mesh SiC, constantly replenished, to ensure a uniform density of nucleating surface flaws for the cone cracks [8]. Care was taken to align the surface-normal of all specimens to within 0.1° of the load axis. With crystalline quartz, mechanical anisotropy was a further important consideration [11]; in the present tests the quartz surfaces were oriented to within 1° of the (0001) plane ("Z-cut").

Preliminary runs were made on some specimens to investigate reproducibility. These runs also served to confirm the basic bond-rupture picture outlined in the Introduction. In general, the critical load to fracture was found to be insensitive to variations in the load rate for tests in vacuum, but not for tests in any environment with water content; in the latter case P_c was depressed, the effect becoming more pronounced with increasing water concentration and load duration. Thermal cycling of the specimens in vacuum indicated that an anneal

TABLE I Values of P_c (N) before and after anneal at 850 K in vacuum. Load rate fixed at $\dot{P} = 2.5$ N sec^{-1}. Each result mean of at least ten tests, with standard deviation.

	Pre-bakeout	Post-bakeout
Quartz (Z-cut)	627 ± 62	626 ± 60
Fused silica	542 ± 31	601 ± 45
Soda-lime glass	947 ± 47	1097 ± 107

for at least 4 h at the upper limit of the temperature range of interest was an advisable precaution (Table I); this ensured the elimination of any spurious effects arising from residual by-products and stresses in the abrasion flaws.

Thus with moderate care in specimen preparation, reproducibility in P_c to better than ± 10% was readily obtainable*. Specimen history subsequent to the initial bakeout cycle was not found to affect the results [9].

2.2. Physical interpretation

In the Hertzian test, as indeed in all fracture tests, it is essential to appreciate what properties of a material are being measured. This, in turn, requires an understanding of the mechanics of cone-crack formation [7-10, 13].

All theories of Hertzian fracture begin with the equation of elastic contact [14]. The relevant parameters are shown in Fig. 2. We consider the case in which the load, P, increases linearly with time, t,

$$P = \dot{P}t \ (\dot{P} \text{ fixed}). \tag{1}$$

At any given load the radius of elastic contact

$$a = \left(\frac{4kr}{3E}\right)^{\frac{1}{3}} P^{\frac{1}{3}} \tag{2}$$

and the mean indentation pressure

$$\sigma_0 = \frac{P}{\pi a^2} = \left(\frac{9E^2}{16\pi^3 k^2 r^2}\right)^{\frac{1}{3}} P^{\frac{1}{3}} \tag{3}$$

determine the scale of the field: the bracket terms are test invariants, with E = Young's modulus of the specimen, r = the indenter radius, and $k \simeq 1$ = a dimensionless term in elastic constants of both indenter and specimen. It is of interest to note the time-averages of Equations 2 and 3:

$$\left.\begin{aligned} \bar{a} &= \frac{1}{t_c}\int_0^{t_c} a(t)\,\mathrm{d}t = \frac{3}{4}\,a_c \\ \bar{\sigma}_0 &= \frac{1}{t_c}\int_0^{t_c} \sigma_0(t)\,\mathrm{d}t = \frac{3}{4}\,\sigma_{0c} \end{aligned}\right\} \tag{4}$$

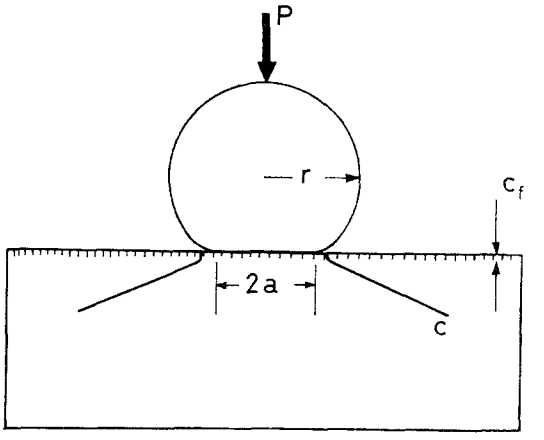

Figure 2 Hertzian test parameters. Cone crack, length c, initiates from surface flaw, length c_f, at critical indenter load P_c.

where the subscript c refers to critical values at the instant of cone-crack formation. Thus the field is near to critical for a large part of the test duration.

The development of the Hertzian cone is governed by the nature of the strongly inhomogeneous stress field beneath the indenter. With increasing load the abrasion flaws outside the contact circle experience an ever-increasing radial tensile stress. At some stage in the loading one of the flaws propagates around the indenter and begins to extend slowly downward into the specimen as a shallow ring crack [15]; typically, for a critical contact radius $a_c \simeq 500$ μm, the ring grows to a depth $\simeq 50$ μm. Upon attaining the critical load the surface ring becomes unstable, and visibly propagates to a depth $c \simeq 500$ μm. In isotropic solids the cone-crack is near-symmetrical about the load axis, the fracture proceeding along a path of maximum tensile stress [7]; whereas in single crystals cleavage tendencies impose a crystallographic character on the geometry [11, 16], the fracture now proceeding along a path subjected to a component of shear. Anisotropy serves only to increase the mathematical complexity of a common theoretical approach, and need not be considered further in this section.

*All data points in subsequent graphs represent the mean of at least ten tests, and error bars are omitted for clarity on the understanding that the standard deviation is generally < 10% of the mean value.

Standard fracture-mechanics routine involves the determination of a convenient crack parameter for direct incorporation into an extension criterion. Such a parameter is the *stress-intensity factor*, K, which relates the intensity of the local stress field about the crack tip to the applied loading [17]. This factor assumes the functional form

$$K = K(\sigma,c) . \tag{5}$$

For a complete solution, K must be evaluated at each point along the ultimate crack path in terms of the Hertzian stress field [7, 16]. The calculation is tedious, and the general case requires a computer [13]. Since K is found to increase monotonically with σ, the time-average $\bar{K}$ is biased toward the critical value K_c at cone fracture in the manner of Equation 4.

In the present instance we are concerned with the time-variation of K associated with the slow growth of the surface ring crack preceding development of the cone. With this information the critical fracture load may be estimated from the relation

$$P_c = \dot{P} t_c = \dot{P} \int_0^{K_c} \mathrm{d}K/\dot{K} . \tag{6}$$

Now at a given instant, K is uniquely determined by the indenter load and crack length, as is evident from Equations 5 and 3. Differentiation then gives

$$\dot{K}(P,c) = \frac{\partial K}{\partial P}\dot{P} + \frac{\partial K}{\partial c}\dot{c} \; ; \tag{7}$$

that is, the stress intensity may be enhanced by variations in either P or c. Sufficient physical insight into the Hertzian problem may be gained without attempting the difficult task of evaluating $\partial K/\partial P$, $\partial K/\partial c$ in Equation 7.

First, we treat the case of cone fracture under environment-free conditions. Our earlier observation that P_c is independent of $\dot{P}$ in vacuum is consistent with either of two possible interpretations of Equations 6 and 7: (i) $\dot{c} = 0$; the surface ring remains stationary in a subcritical state until an unstable equilibrium is ultimately attained, at which point the ring propagates into the cone; (ii) $\dot{c} \propto \dot{P}$ (although the "constant" of proportionality may itself be a function of c, P); i.e. the surface ring grows downward in a stable manner before instability, at a rate governed by the load rate. Of the two possibilities, the second is favoured by detailed analysis [7, 8]. In either case the surface ring is in equilibrium at $K = K_c$ immediately prior to the sudden growth of the cone. Thus the critical condition may be predicted in terms of the fundamental Griffith condition for crack equilibrium [1], which leads to a direct relationship between K_c and the energy, γ, per unit area of new fracture surface [17]. From the analysis emerges the simple result $P_c \propto \gamma$; the proportionality constant, although independent of elastic moduli, is highly sensitive to Poisson's ratio, and cannot be estimated with much better than order-of-magnitude accuracy. Thus the critical load in vacuum is ideally suited to measuring variations in the intrinsic surface energy of highly brittle solids as the conditions of testing (e.g. temperature) are changed; however, because of the uncertainty in absolute values, comparative measurements on different materials (e.g. Table I) should not be taken as a reliable indication of relative strengths.

Second, we consider the modifications in cone-crack behaviour on admitting a chemical environment. If the interaction between chemical species and crack tip were to be instantaneous, the observed depression of P_c might be ascribed to a lowering of surface energy [18]. However, the time-dependence of P_c indicates that the approach to a new equilibrium occurs at a finite rate, so that the surface ring grows subcritically according to some kinetic equation, $\dot{c} = \dot{c}(K)$; until Griffith equilibrium at $K = K_c$ is once more exceeded. Thus, at a given load rate, the environmental interaction acts to increase the magnitude of $\dot{c}$ in Equation 7, hence also of $\dot{K}$, so that Equation 6 predicts premature failure. Moreover, as $\dot{P}$ is reduced, the second term in Equation 7 begins to dominate, and the predicted reduction in P_c becomes more pronounced. The depression in critical load may therefore be taken as a measure of the rate processes responsible for subcritical crack growth.

Third, we may note that the Griffith equilibrium condition strictly relates the critical stress-intensity factor, K_c, to the intrinsic surface energy, γ, for a given solid. Now if irreversible processes occur in the near-vicinity of the crack tip, additional energy may be expended in creating new fracture surface [19], with a consequent increase in K_c. The attendant increase in P_c in Equation 6 would then reflect the magnitude of any such dissipative process.

3. Tests in vacuum

3.1. Results

The variation of P_c with temperature for vacuum runs at two load rates is shown in Fig. 3. Neither quartz nor fused silica shows evidence of load-rate effects over the temperature range studied, but soda-lime glass shows an *increase* in P_c with decreasing load rate at elevated temperatures. Examination of the test surfaces revealed the "tail" in the soda-lime glass curve to be associated with extensive viscous flow in the specimen beneath the indenter; indeed, above about 800 K no cone-crack could be produced at all, the indenter merely embedding itself in the glass surface. In no case was there any *depression* of P_c arising from the presence of residual water in the system.

The feature of greatest significance in Fig. 3 is the marked difference in behaviour between the crystalline and amorphous modifications. At the lower end of the temperature range all three materials show an initial decline in strength, followed by a tendency to level out. However, at the upper end of the range the curve for quartz displays a dramatic plunge to near-zero strength at the $\alpha \rightarrow \beta$ transition temperature. The curious dip in the quartz curve at 450 K was found to be a real effect present in all specimens tested.

The above results appear to be consistent with the limited strength-temperature data in the literature. Ernsberger [3], in reviewing the available evidence on inorganic glasses, and Hartley and Wilshaw [11], in reporting on Hertzian fracture data from tests on α-quartz in a dry nitrogen environment, describe trends similar to those observed in Fig. 3. However, as these authors are careful to point out, lack of control in test procedure has led to ambiguity in interpretation. In particular, extreme sensitivity of fracture data to surface conditions often tends to obscure intrinsic strength characteristics. No such extraneous effects are apparent in the curves of Fig. 3, where $P_c(T)$ is seen to be independent of specimen history and load duration (the soda-glass "tail" excepted).

3.2. Thermal effects in the silica structure

Granted that the data in Fig. 3 truly reflect the intrinsic strength of the silica structures, it is clear that temperature is an important variable. Moreover, since the crystalline and amorphous phases differ so widely in their temperature response, one is led to seek a thermodynamic

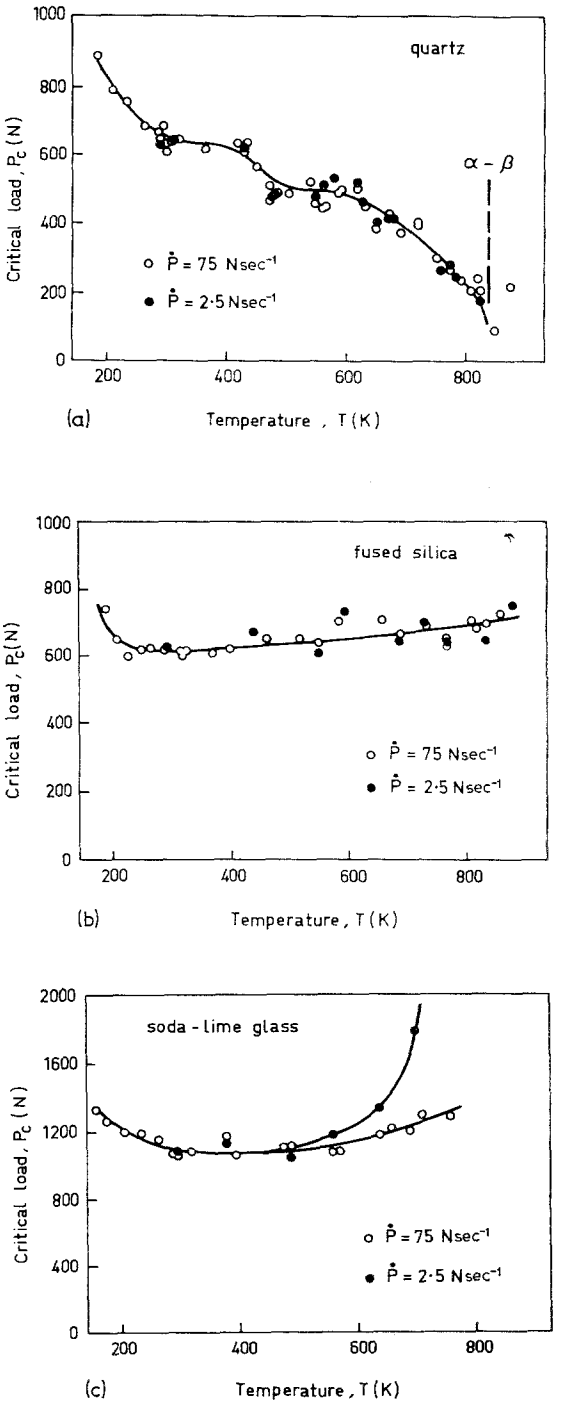

Figure 3 Hertzian strength of quartz (Z-cut), fused silica and soda-lime glass as function of temperature in vacuum. Data taken during heating and cooling cycle (after anneal).

model in terms of *differences* rather than *similarities* in the structures. Attention therefore turns from the Si-O bridging bond to the SiO_4^{4-} tetrahedral stacking unit.

The structures of silica are complex, but the schematic representations in Fig. 4 serve to illustrate the distinguishing features [20-22]. The diagram shows only silicon atoms, and oxygen atoms are to be envisaged as linking each pair of silicons. On heating quartz through the $\alpha \rightarrow \beta$ inversion temperature a rapid, reversible, displacive transformation takes place. If the crystal is further heated beyond its melting point, and then cooled rapidly, the disordered, "supercooled liquid" state of fused silica is retained. In all transformations the tetrahedral unit remains intact, with the –Si–O–Si– bond linkage undergoing angular distortions. The additional modifications to the network structure which arise from compositional changes in inorganic glasses are of secondary importance here, and will be taken up in the following section.

Various physical properties provide a clear indication of the above structural differences in their temperature curves. The behaviour is exemplified by the specific heat (Fig. 5). The gradual rise in the quartz curve to the discontinuity at the $\alpha \rightarrow \beta$ inversion temperature is characteristic of a second-order phase transition [24]; this is suggestive of a rapidly increasing conversion from an ordered to disordered state in the vibrational modes of the tetrahedra. Similar anomalous increases are observed in the thermal expansion coefficients [25] and elastic compliances [26]; thus, although Si–O linkage bonds are not broken in the $\alpha \rightarrow \beta$ inversion, there is a strong indication that they are severely stretched. Of course, no such anomalies are apparent in fused silica, in which the degree of configurational disorder in the tetrahedral stacking is virtually complete over the entire temperature range.

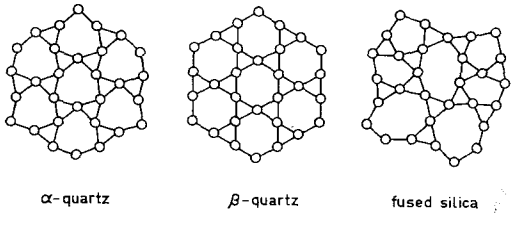

Figure 4 Projected structures of the modifications of SiO_2. Only the silicon atoms are shown, and bonds joining adjacent atoms are inclined to the plane of the drawing.

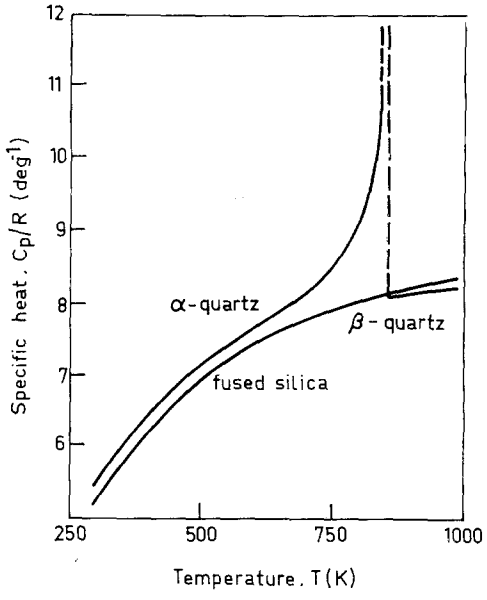

Figure 5 Specific heat of quartz and fused silica. Note anomaly in quartz curve prior to $\alpha \rightarrow \beta$ transition (846 K). (After Moser [23].)

We now have the basis for a simple extension of the bond-rupture model of brittle fracture. Taking the bonds to be highly directional and short-ranged in nature, the surface energy may be approximated as

$$2\gamma = N_A U_B , \qquad (8)$$

where N_A is the number of bonds intersecting unit area of crack plane (see Fig. 6), and U_B is the energy needed to "break" one bond. This link between surface energy and nearest-neighbour bond energy is doubtless a tenuous one, for the Si–O bond has a substantial polar character [27], but one may reasonably presume the curves in

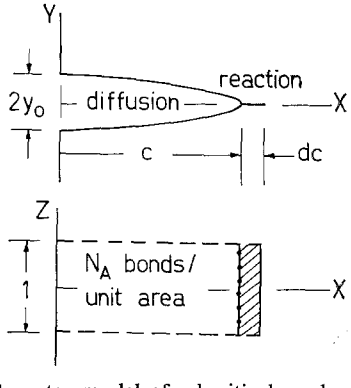

Figure 6 Two-step model of subcritical crack growth.

Fig. 3 to reflect the temperature dependence of the work term involved in separating atoms across the crack plane. Then, as quartz is heated through the $\alpha \rightarrow \beta$ transition, the SiO_4^{4-} tetrahedra undergo oscillations of increasing amplitude, and the –Si–O–Si– bridges begin to elongate. Less work is required to separate bonds across the crack plane, and the critical fracture load consequently falls.

3.3. Composition and deformation effects

The above treatment deals with inherent thermal properties of the silica network, and indicates these to be of primary importance in characterizing strength variations under environment-free conditions. But other factors relating to local departures from the idealized linked-tetrahedron picture have been discussed in the literature, and, although apparently of minor significance in the present results, warrant brief consideration.

First, the "open" silica structure can accommodate a high concentration of an additive oxide component, as with the soda-glass system Na_2O-SiO_2. Oxygen atoms may then associate with the cations, e.g., sodium, located in interstitial sites, to form "terminal bonds", thereby disrupting the bridging network. It may reasonably be argued that the relative number of terminal and bridging bonds intersecting an arbitrary crack plane will be in proportion to composition, in which case intrinsic strength differences of considerably less than a factor of two should occur over an extreme range of silicate glass compositions. Wiederhorn [28] has shown this to be the case. Moreover, the bond-count argument would appear to be equally applicable at all temperatures, in accord with the near-constant strength difference between fused silica and glass (lower curve) in Figs. 3b and c.

On the other hand, if the interstitial species is mobile the effects may be more far-reaching. In particular, kinetic terms will enter into consideration, and temperature and time will become important variables. The low viscosity of inorganic glasses is a notable example of an impurity-activated process [6, 29], and accounts for the tail in the lower load-rate curve for glass (upper curve) in Fig. 3c; the flow provides stress relief, particularly in the vicinity of the crack tip, thus increasing the work to fracture. An opposite effect, in which stress-enhanced diffusion of trace impurities (especially water) to the crack tip lowers the work to fracture, has been suggested as a possible explanation of the strength decline with temperature in quartz [11] and fused silica [30]. But the absence of the rate-dependent effects in the appropriate curves of Fig. 3 rules out this possibility as a viable mechanism in the present experiments.

Further, mechanisms involving plasticity cannot be overlooked. Marsh [19] has proposed local crack-tip yield as the principal strength-determining factor in inorganic glasses, but Ernsberger [3] has produced counter-arguments. Both appear to agree that plasticity is absent in fused silica. In quartz, Griggs and co-workers [31, 32] have observed thermally activated yield below the inversion temperature, and Shubnikov and Zinserling [33] have described the formation of twins in ball-indentation tests. However, in no instance has it been made clear how any plasticity mechanism might contribute to a lowering of the equilibrium work to fracture.

One detail which has no obvious explanation in terms of any mechanism yet discussed is the slight dip in the quartz curve in Fig. 3a at about 450 K. Whether this dip arises from a minor anomaly in the quartz structure or merely from some spurious cause remains an issue for further study.

4. Tests in water environment

4.1. Results

A second series of experiments was aimed at investigating the profound influence of a water environment on the fracture properties of the silica materials. Figs. 7 to 9 demonstrate the important parameters, namely load rate, temperature, chemical concentration (pressure) of H_2O, and physical state of environment.

Fig. 7 serves to illustrate the general behaviour. Fused silica, because of its uncomplicated temperature response in vacuum, shows the environmental influence to best advantage. Several features are readily apparent: (i) The presence of water leads to substantial reductions in P_c, these reductions increasing with decrease in load rate; (ii) the depression in P_c increases with increasing chemical concentration, i.e. in proceeding from the vapour to the liquid phase; (iii) temperature has a negligible effect on results in the vapour environment, but notably enhances the weakening in the liquid environment. These observations indicate the operation of at least one kinetic process in the crack growth.

The results from a comparison run on all three silica modifications in water (liquid phase)

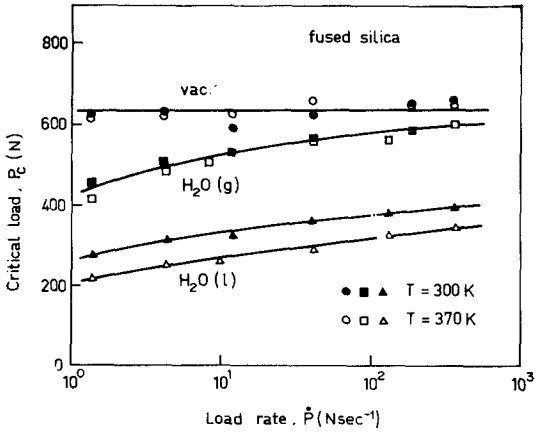

Figure 7 Hertzian strength of fused silica as function of load rate. Vacuum and water environments at two temperatures. (Pressure in water vapour environment 260 N m^{-2}.)

TABLE II Values of P_c (N) in vacuum and water (liquid) environment. Tests at 300 K, $\dot{P}$ = 2.5 N sec^{-1}.

	Vacuum	H_2O (*l*)
Quartz (Z-cut)	652 ± 56	402 ± 35
Fused silica	610 ± 60	351 ± 21
Soda-lime glass	1053 ± 86	439 ± 32

(Table II) confirm the universality of the SiO_2–H_2O interaction. In each case the strength is reduced by a factor of about one half, although this factor does increase slightly down the table. The role of composition and structure of the silica network therefore seems to be of secondary importance here.

A closer look at the role of chemical concentration of the environment is presented in Fig. 8. These data, taken from a test run on soda-lime glass in water vapour at room temperature, emphasize the potency of the interaction. At the slower load rates, hydrolytic weakening is detectable under conditions which might normally be considered to constitute a "moderate" vacuum.

Finally, temperature variations are given detailed attention in Fig. 9. Each of the silica materials has been tested under dilute gas conditions. Again, as in Fig. 7, heating does not enhance the hydrolytic weakening when the water exists in the *vapour* phase. Similar attention was not extended to tests in a *liquid* environment, firstly because the positive temperature effect noted in Fig. 7 had been investigated in some detail in a previous paper [9], and secondly for

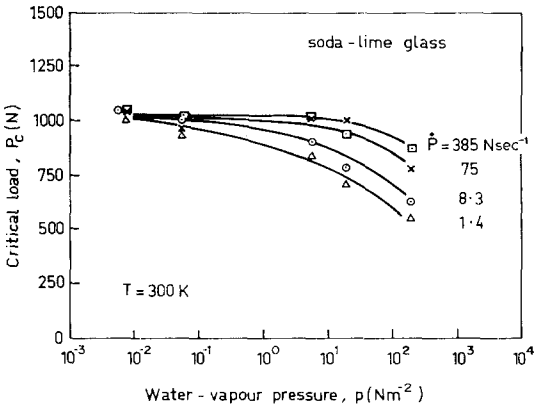

Figure 8 Hertzian strength of soda-lime glass as function of water-vapour pressure. Room-temperature run at four load rates. (1 N m^{-2} ≡ 10^{-2} Torr.)

the more practical reason that water cannot exist in its liquid phase over the entire temperature range of interest (except under a confining pressure of several hundred atmospheres).

The phenomenon of environment-induced cracking has been extensively studied in glasses (see Wiederhorn's review [5]), although work on quartz is only just beginning to appear [34, 35]. Most of the above results conform to the established pattern of behaviour. However, the widely differing influence of gas and liquid environments on the temperature dependence of P_c is one aspect of the present findings which has largely gone unnoticed.

4.2. The role of reaction and diffusion kinetics

It was pointed out in Section 2.2 that the depression in P_c arising from admittance of a reactive environment gives a measure of the kinetic processes involved in subcritical crack growth. The basic chemical reaction between siloxane bonds at the crack tip and impinging water molecules is

$$H_2O + (\text{–Si–O–Si–}) \rightarrow (\text{–Si–OH . HO–Si–}) \quad (9)$$

That is, the strongly bonded bridging oxygen is replaced by two weakly coupled (hydrogen bonded) hydroxyls, thereby facilitating crack extension at subcritical stress intensities. The question then arises: if this simple bond-rupture description is correct, why are the kinetics of crack growth as reflected in the Hertzian fracture data so dependent on the *state* of the water environment?

A satisfactory explanation follows if it is postulated that at least one other kinetic step

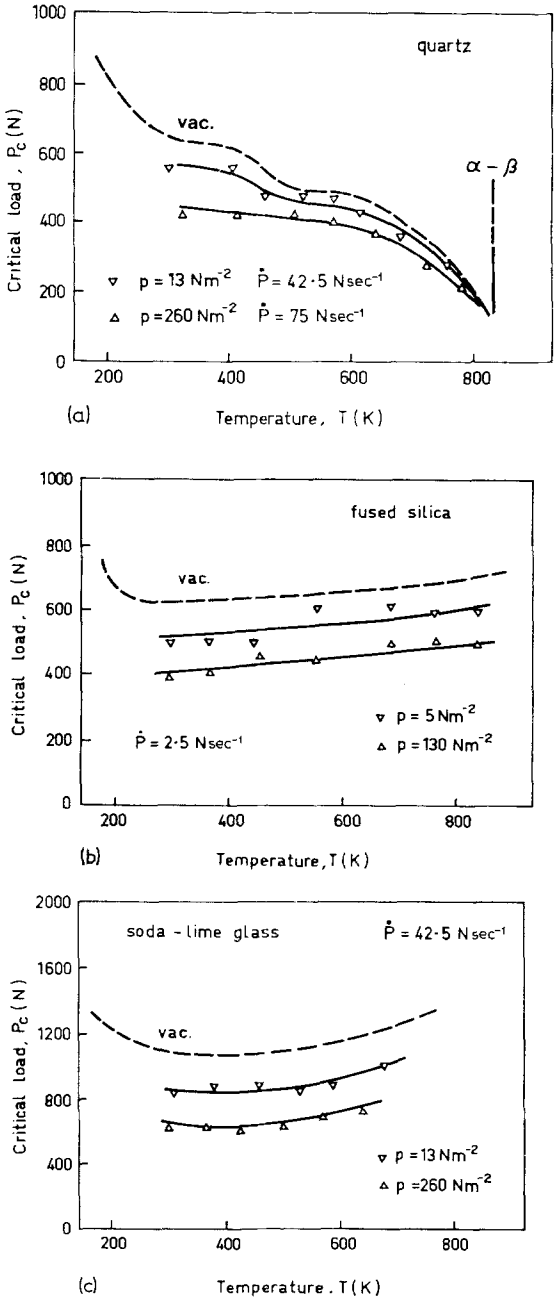

Figure 9 Hertzian strength of quartz (Z-cut), fused silica and soda-lime glass as function of temperature in water vapour (two pressures). Vacuum curve from Fig. 3. Load rate fixed for each run.

precedes the crack-tip reaction. The existence of a sequence of essential steps is in fact common in chemical reactions, and the slowest of these steps will control the rate of the overall process [36]. It is, therefore, possible that different rate-controlling steps may be operative in gas and liquid environments, each varying with the environmental fracture parameters in its own characteristic manner. Now, the typically narrow separation between crack walls in the highly brittle solids investigated here strongly suggests that transport mechanisms may limit the supply rate of chemical material to the active crack-tip zone; moreover, such mechanisms should be sensitive to the state of the environment. One is led to try for a simple two-step, diffusion-reaction kinetic model.

A model along these lines has been developed elsewhere [37], and only the relevant details need to be presented here. Suppose we consider the crack of length c, width unity, in Fig. 6. The number of crack-tip bonds ruptured in an incremental extension is $dN = N_A\, dc$, leading to a crack advance rate

$$\dot{c} = \frac{dc}{dt} = \frac{1}{N_A}\frac{dN}{dt}. \tag{10}$$

The problem, therefore, reduces to one of relating the bond-rupture rate dN/dt to the parameters of the rate-controlling step. We treat the reaction and diffusion steps separately.

4.2.1. Reaction-control

In a reaction-controlled process the bond-rupture rate may be calculated from the theory of absolute reaction rates [36]. The resulting crack-velocity equation is of the form [4]

$$\dot{c} = v_r(p,T,K) = v_{ro}(p,T)\exp\left(\frac{-E^* + bK}{kT}\right) \tag{11}$$

with p a chemical concentration parameter (e.g. gas pressure), T the absolute temperature, K the stress-intensity factor, E^* an activation energy for the reaction, bK a term designating stress-induced lowering of the activation barrier, and k the Boltzman constant; $v_{ro}(p.T)$ is a slowly-increasing function of concentration and temperature. The constants in this equation have been determined empirically by Wiederhorn and Bolz [38] for several glasses in a water environment.

4.2.2. Diffusion-control

In a diffusion-controlled process the crack velocity follows from an appropriate transport equation. For a dense fluid (the terms "dense" or "dilute" applying according to whether the interatomic collision distance in the fluid is much less or greater than the crack-wall separation)

capillary flow along the fracture interface is limited by viscous forces [39]; however, these forces appear to have little restrictive effect on subcritical crack velocities in the system SiO_2-$H_2O(l)$ [40, 41]. For a dilute gas, on the other hand, considerably greater flow attenuation may arise from retarding molecule-wall collisions ("free molecular flow") [42] as the crack tip is approached; this attenuation is clearly apparent in the crack velocity data for the system SiO_2-H_2O(g) [40, 41]. The appropriate crack-velocity equation for diffusion-control in a gaseous environment is of the form [37]

$$\dot{c} = v_d(p,T,K) = \text{const.}\, pT^{-\frac{1}{2}}K^2 \,. \qquad (12)$$

Equations 11 and 12 contain the key to the different temperature dependence of the Hertzian fracture load in liquid and gas environments. With the liquid, where transport processes are comparatively rapid, subcritical crack growth is governed almost entirely by Equation 11. Small temperature increases therefore significantly enhance $\dot{c}$, and lead to a corresponding decrease in P_c. With the gas, the rate-controlling step is determined by the smaller of the two quantities v_r, v_d. Since the time-average of K is large in the Hertzian test when the load rate is constant (Section 2.2), we expect $v_r \gg v_d$ for the greater part of the experiment. Under these conditions Equation 12 governs. Temperature variations then have little effect on $\dot{c}$, and P_c simply follows the same trends as observed in vacuum [37].

4.3. Other factors in subcritical crack growth

The above results clearly demonstrate the environmental state to be an important factor supplementary to the basic variables load rate, temperature and concentration. Other subsidiary factors have been established under conditions of fracture somewhat different to those considered here; these bear on the question of the overall applicability of the Hertzian method as a fracture tool.

It was mentioned in Section 3.3 that mobile ions in the silica network are capable of exerting a strong influence on mechanical properties. This is certainly evident in the crack-velocity data of Wiederhorn and Bolz [38]; in particular, the (reaction-controlled) crack velocities for soda-lime glass and fused silica in water differ by several orders of magnitude at low K, but tend to merge as $K \to K_c$. Because the present test arrangement is biased toward larger values of K, this large composition effect appears only as a minor perturbation in Table II.

Again, similar effects may arise from the presence of an additional component in the environment. Thus, for instance, Wiederhorn and Johnson [43] have found crack velocities in glasses to vary strongly with pH of aqueous solution. Their results for soda-lime glass diverge most noticeably at large K, in accord with the pronounced influence of pH on Hertzian strength observed by Langitan and Lawn [91]. The widely differing sensitivity of P_c to chemical effects in this and the previous example cited demonstrates a limitation of the Hertzian test in its constant load-rate mode.

Returning finally to the possibility of plasticity at the crack tip (Section 3.3), it has been proposed that water-induced softening may be an important factor facilitating subcritical crack extension in inorganic glasses [44]. An interesting extension of this concept has recently been considered by Westwood and Huntington [45] in connection with fracture tests in surfactant solutions; in fact, surfactants may profoundly affect Hertzian strength values [46]. However, direct confirmation of softening mechanisms is not yet at hand, and the proposal remains one of some controversy.

5. Concluding remarks

The present comparative study of the various silica materials illustrates the general usefulness of the Hertzian test as a means for investigating the important parameters controlling fracture strength. From this study emerges the need to supplement the simple Si–O bond-rupture concept of fracture with an account of the thermal properties of the silica tetrahedra, and the physical state of the environment.

On the debit side, however, the tendency for the test in its present form to reflect crack-velocity characteristics at near-critical stress-intensity factors represents a severe limitation of the technique, and may lead to the oversight of certain variables. It is clear that one should be fully conversant with the fracture mechanics of the Hertzian test (indeed, of any fracture test) before assessing the results in terms of any given model. In this respect, experimental arrangements which provide facility for direct recording of instantaneous crack velocities at all stages of growth (e.g. cantilever tests [4, 5]) have a clear advantage over those which merely relate to

some time-averaged value (although, of course, only at great expense in simplicity). Current work is aimed at extending the Hertzian test facility to allow detailed observations of the growing cone.

A final comment may be made about quartz, the silica modification which has received least attention in the literature but which is of greatest geophysical importance. Our tests have been conducted under conditions of time, temperature and pressure barely touching on those prevailing beneath the earth's surface, and it is more than possible that some of the mechanisms regarded here as being of secondary importance may play a crucial role in geological processes. For example, hydrolytic weakening resulting specifically from stress-induced diffusion of interstitial water to the crack tip [11] was not considered to be a significant factor in Fig. 3; yet Griggs [32] presents compelling evidence for an analogous mechanism in relation to dislocation motion in yield tests under confining pressures. Long-term observations of crack growth at constant load may be needed to resolve the question of the existence of such mechanisms.

Acknowledgements

We are indebted to T. R. Wilshaw and N. E. W. Hartley, who motivated the present work on quartz and who supplied the Z-cut specimens (originally grown by the Sawyer Research Corporation, USA). We are also grateful to A. R. C. Westwood and R. D. Huntington, and to S. M. Wiederhorn, for access to results prior to publication. The receipt of Commonwealth Scholarships by the first two authors is acknowledged.

References

1. A. A. GRIFFITH, *Phil. Trans.* **A221** (1920) 163.
2. R. E. MOULD, "Fundamental Phenomena in the Materials Sciences", Vol. 4 (Plenum Press, New York, 1967) p. 119.
3. F. M. ERNSBERGER, Proceedings of the Eighth International Congress on Glass (1968) p. 123.
4. S. M. WIEDERHORN, "Mechanical and Thermal Properties of Ceramics", ed. J. B. Wachtman Jun. (N.B.S. Special Publications, 303, 1969) p. 217.
5. *Idem*, "Proceedings of the International Conference on Corrosion Fatigue" (University of Connecticut, 1971, to be published).
6. G. O. JONES, "Glass", 2nd Edn. (Chapman and Hall, London, 1971).
7. F. C. FRANK and B. R. LAWN, *Proc. Roy. Soc.* **A299** (1967) 291.
8. F. B. LANGITAN and B. R. LAWN, *J. Appl. Phys.* **40** (1969) 4009.
9. *Idem, ibid* **41** (1970) 3357.
10. T. R. WILSHAW, *J. Phys. D: Appl. Phys.* **4** (1971) 1567.
11. N. E. W. HARTLEY and T. R. WILSHAW, *J. Mater. Sci.* **8** (1973) 265.
12. J. J. H. BEEK and B. R. LAWN, *J. Phys. E: Sci. Instrum.* **5** (1972) 710.
13. B. R. LAWN, N. E. W. HARTLEY, and T. R. WILSHAW, *Internat. J. Fract. Mech.* (in press).
14. H. HERTZ, "Miscellaneous Papers" (Macmillan, London, 1896) chs. 5, 6.
15. A. G. MIKOSZA and B. R. LAWN, *J. Appl. Phys.* **42** (1971) 5540.
16. B. R. LAWN, *ibid* **39** (1968) 4828.
17. P. C. PARIS and G. C. SIH, "Fracture Toughness Testing and its Applications", ASTM Special Technical Publication No. 381 (1965) p. 30.
18. E. OROWAN, *Nature* **154** (1944) 341.
19. D. M. MARSH, *Proc. Roy. Soc.* **A282** (1964) 33.
20. L. BRAGG and G. F. CLARINGBULL, "Crystal Structures of Minerals" (Bell, London, 1965) ch 6.
21. W. H. ZACHARIASEN, *J. Amer. Chem. Soc.* **54** (1932) 3841.
22. B. E. WARREN, *J. Appl. Phys.* **8** (1937) 645.
23. H. MOSER, *Physik. Z.* **37** (1936) 737.
24. J. C. SLATER, "Introduction to Chemical Physics" (McGraw-Hill, New York, 1939) ch. 18.
25. A. H. JAY, *Proc. Roy. Soc.* **A142** (1933) 237.
26. A. PERRIER and R. de MANDROT, *Mem. Soc. Vaud. des Sciences Nat.* **7** (1923) 333.
27. F. C. FRANK and J. W. HEAVENS, unpublished work.
28. S. M. WEIDERHORN, NBS Report 10892 (1972).
29. G. HETHERINGTON, K. H. JACK, and J. C. KENNEDY, *Phys. Chem. Glasses* **5** (1964) 130.
30. B. A. PROCTOR, I. WHITNEY, and J. W. JOHNSON, *Proc. Roy. Soc.* **A297** (1967) 534.
31. D. T. GRIGGS and J. D. BLACIC, *Science* **147** (1965) 292.
32. D. T GRIGGS, *Geophys. J. Roy. Astron. Soc.* **14** (1967) 19.
33. A. V. SHUBNIKOV and K. ZINSERLING, *Z. Krist.* **83** (1932) 243.
34. R. J. MARTIN III, *J. Geophys. Res.* **77** (1972) 1406.
35. C. H. SCHOLZ, *ibid* **77** (1972) 2104.
36. S. GLASSTONE, K. J. LAIDLER, and H. EYRING, "The Theory of Rate Processes" (McGraw-Hill, New York, 1941).
37. B. R. LAWN, to be published.
38. S. M. WIEDERHORN and L. H. BOLZ, *J. Amer. Ceram. Soc.* **53** (1970) 543.
39. A. W. ADAMSON, "Physical Chemistry of Surfaces" (Interscience, New York, 1967) ch. 10.
40. S. M. WIEDERHORN, *J. Amer. Ceram. Soc.* **50** (1967) 407.

41. K. SCHÖNERT, H. UMHAUER, and W. KLEMM, Proc. Second Internat. Conf. Fracture, Brighton, 1969 (Chapman and Hall, London 1969) paper 41.
42. M. KNUDSEN, "The Kinetic Theory of Gases" (Methuen, London, 1950).
43. S. M. WIEDERHORN and H. JOHNSON, NBS Report 10890 (1972).
44. K. R. LINGER and D. G. HOLLOWAY, *Phil. Mag.* **18** (1968) 1269.
45. A. R. C. WESTWOOD and R. D. HUNTINGTON, Proceedings Internat. Conf. Mechanical Behaviour of Materials (Kyoto, 1971).
46. A. R. C. WESTWOOD and R. D. HUNTINGTON, unpublished work.

Received 19 December 1972 and accepted 22 January 1973.